

ROYAL SOCIETY
OPEN SCIENCEroyalsocietypublishing.org/journal/rsos

Research



Cite this article: Whittaker DG, Capel RA, Hendrix M, Chan XHS, Herring N, White NJ, Mirams GR, Burton R-AB. 2021 Cardiac TdP risk stratification modelling of anti-infective compounds including chloroquine and hydroxychloroquine. *R. Soc. Open Sci.* **8**: 210235. <https://doi.org/10.1098/rsos.210235>

Received: 9 February 2021

Accepted: 30 March 2021

Subject Category:

Organismal and evolutionary biology

Subject Areas:

computational biology/biophysics

Keywords:

arrhythmia, electrophysiology, computational biology, pharmacology

Author for correspondence:

Rebecca-Ann B. Burton

e-mail: rebecca.burton@pharm.ox.ac.uk


†Joint senior authors.

Electronic supplementary material is available online at rs.figshare.com.

Cardiac TdP risk stratification modelling of anti-infective compounds including chloroquine and hydroxychloroquine

Dominic G. Whittaker¹, Rebecca A. Capel², Maurice Hendrix^{1,3}, Xin Hui S. Chan^{4,5}, Neil Herring⁶, Nicholas J. White^{4,5}, Gary R. Mirams^{1,†} and Rebecca-Ann B. Burton^{2,†}

¹Centre for Mathematical Medicine and Biology, School of Mathematical Sciences, University of Nottingham, Nottingham, UK²Department of Pharmacology, University of Oxford, Oxford, UK³Digital Research Service, University of Nottingham, Nottingham, UK⁴Mahidol-Oxford Tropical Medicine Research Unit, Mahidol University, Bangkok, Thailand⁵Centre for Tropical Medicine and Global Health, Nuffield Department of Medicine, University of Oxford, Oxford, UK⁶Department of Physiology, Anatomy and Genetics, University of Oxford, Oxford, UK

 **id** DGW, [0000-0002-2757-5491](https://orcid.org/0000-0002-2757-5491); MH, [0000-0002-6621-7996](https://orcid.org/0000-0002-6621-7996); XHSC, [0000-0002-9941-6975](https://orcid.org/0000-0002-9941-6975); GRM, [0000-0002-4569-4312](https://orcid.org/0000-0002-4569-4312); R-ABB, [0000-0002-0904-3862](https://orcid.org/0000-0002-0904-3862)

Hydroxychloroquine (HCQ), the hydroxyl derivative of chloroquine (CQ), is widely used in the treatment of rheumatological conditions (systemic lupus erythematosus, rheumatoid arthritis) and is being studied for the treatment and prevention of COVID-19. Here, we investigate through mathematical modelling the safety profile of HCQ, CQ and other QT-prolonging anti-infective agents to determine their risk categories for *Torsade de Pointes* (TdP) arrhythmia. We performed safety modelling with uncertainty quantification using a risk classifier based on the qNet *torsade metric score*, a measure of the net charge carried by major currents during the action potential under inhibition of multiple ion channels by a compound. Modelling results for HCQ at a maximum free therapeutic plasma concentration (free C_{\max}) of approximately 1.2 μM (malaria dosing) indicated it is most likely to be in the high-intermediate-risk category for TdP, whereas CQ at a free C_{\max} of approximately 0.7 μM was predicted to most likely lie in the intermediate-risk category. Combining HCQ with the

antibacterial moxifloxacin or the anti-malarial halofantrine (HAL) increased the degree of human ventricular action potential duration prolongation at some or all concentrations investigated, and was predicted to increase risk compared to HCQ alone. The combination of HCQ/HAL was predicted to be the riskiest for the free C_{\max} values investigated, whereas azithromycin administered individually was predicted to pose the lowest risk. Our simulation approach highlights that the torsadogenic potentials of HCQ, CQ and other QT-prolonging anti-infectives used in COVID-19 prevention and treatment increase with concentration and in combination with other QT-prolonging drugs.

1. Introduction

The cinchona alkaloid quinine (QUIN), along with synthetically produced chloroquine (CQ), are quinoline compounds which have been used in the treatment of malaria for decades. The more soluble hydroxy derivative of CQ is hydroxychloroquine (HCQ). CQ and HCQ are diprotic bases which accumulate in acid vesicles including lysosomes over time. Many of their multiple biological activities including their antiviral action are associated with increased vesicle pH [1]. Both drugs have been shown to block various cardiac ion channels [2].

HCQ was initially developed as an anti-malarial drug, sold as the sulfate salt under the trade name Plaquenil [3]. HCQ is used for the treatment of a wide variety of conditions with the majority of use being for systemic lupus erythematosus (SLE) and rheumatoid arthritis (RA). For these indications, it is often prescribed for use over months to years, and has had a good safety record including in pregnancy [1].

Early clinical studies reported few toxic side effects across HCQ anti-malarial treatment regimens [4]. Work in the late 1950s [5] explored the possibility of using 4-aminoquinolines in the treatment of cardiac arrhythmias, although the specific action of reducing heart rate was not explored. Sumpter *et al.* [6] showed evidence for risk of cardiomyopathy during long-term exposure to high doses of HCQ for the treatment of patients with SLE and RA. The present treatment regime for SLE (generally 200–400 mg d⁻¹) [7] includes doses lower than the one originally used to treat arthritis or malaria [8]. Irreversible retinal toxicity is rare at current recommended doses [9,10]. Reported side effects have been seen in greater than 1000 mg d⁻¹ dosage ranges [11–13]. The risk of retinopathy is increased with large cumulative doses of HCQ (greater than 1000 g) [14]. The arrhythmogenic cardiotoxicity of the quinoline and structurally related anti-malarial drugs are well documented [15]; in particular, effects on hypotension and electrocardiographic QT interval prolongation have been reported. Capel *et al.* [16] in 2015 showed that HCQ also inhibits the pacemaking current I_f and offers the potential of being used as a bradycardic agent. They also noted additional effects on the *L-type calcium channels* and *delayed rectifier potassium channels* in isolated guinea pig sinoatrial node cells, indicating multi-ion channel block in cardiac cells. With the increased re-purposing of CQ and HCQ [14], including for the treatment (SOLIDARITY trial, ISRCTN83971151 and UK RECOVERY trial, ISRCTN50189673) and prevention of COVID-19, there is a need to critically assess the cardiovascular safety profiles of these anti-malarials.

Since the advent of mathematical modelling of cardiac cell activity in the 1960s [17], major new insights have emerged in the field, along with approaches to calibrating such models from experimental data [18], and recognition of the need to quantify uncertainty in predictions [19]. Mathematical modelling has since been shown to be useful in elucidating the requirements for reliable risk assessment predictions, such as the need to account for the actions of compounds on multiple ion channels [20], and has helped to guide experimental design considerations for ion channel screening experiments [21,22].

Prolongation of the QT interval on the surface electrocardiogram (ECG) is a surrogate measurement of prolonged ventricular action potential duration (APD). Dispersion of repolarization (DR) is a result of heterogeneous lengthening of APD throughout the ventricular myocardium, often across the ventricular walls. This DR and the tendency of prolonged APD associated with early afterdepolarizations (EADs) provide the substrate of polymorphic ventricular tachyarrhythmia (VT) associated with long QT syndrome (LQTS) [23], *Torsade de Pointes* (TdP) VT [24]. The vast majority of acquired LQTS cases (which are more prevalent than congenital LQTS cases) are the results of electrolyte abnormalities [25] or adverse drug effects [26], the latter particularly due to interaction with the human Ether-à-go-go-Related Gene (hERG), which encodes the pore-forming subunits (Kv11.1) of the channel carrying the rapidly activating delayed rectifier current, I_{Kr} .

In drug development, hERG IC₅₀ value estimates are used in the pre-clinical assessment of TdP risk. Redfern *et al.* [27] proposed [hERG IC₅₀/EFTPC_{max}] as an improvement over the simplified [hERG IC₅₀].

Mirams *et al.* [20] showed a simulated evaluation of multi-channel effects at the whole-cell level could be used to improve this early prediction of TdP risk. The comprehensive *in vitro* proarrhythmia assay (CiPA) initiative was later established as a novel cardiac safety screening paradigm that takes into account multi-channel drug effects intended to replace the former regulatory strategy which relied on hERG block and QT prolongation, sensitive predictors of TdP which lack specificity [28].

In patients with compromised organ function, such as in COVID-19, understanding drug safety and drug interactions is critical. In this study, we use a computational approach, based on a classifier developed by the CiPA initiative [29], to predict the clinical torsadogenic risk categories associated with CQ, HCQ and other commonly used anti-infective agents known to prolong the QT interval. We also use an independent block model to assess the safety profile of combination therapies and show that torsadogenic potentials of HCQ, CQ and other QT-prolonging anti-infectives used in COVID-19 prevention and treatment increase with concentration and in combination with other QT-prolonging drugs. Although the interest in CQ and HCQ for COVID-19 prophylaxis/treatment has waned, it is hoped that our approach may be considered for the screening of potential future therapies/combination therapies.

2. Methods

In 2015, we showed that HCQ inhibits I_f , L-type calcium channels, and slow and rapid delayed rectifier potassium channels in isolated guinea pig sinoatrial node cells [16]. Five minutes of exposure to 3 μM HCQ conveyed a statistically significant reduction in I_{CaL} ($12 \pm 4\%$ reduction in max. conductance, $n = 6$) and I_{Kr} ($35 \pm 4\%$ reduction across step lengths rendering maximal current activation, $n = 5$) at $p < 0.05$, analysed using repeated-measures ANOVA. We used these data to approximate $\text{IC}_{50\text{s}}$ for the actions of HCQ on I_{Kr} , I_{CaL} and I_{Ks} by fitting the parameters of a Hill curve (assuming a Hill coefficient of 1 [20]). HCQ blocked channels in the following order of potency: $I_{\text{Kr}} > I_{\text{Ks}} > I_{\text{CaL}}$. IC_{50} values for other anti-infective compounds of interest including azithromycin (AZ), chloroquine (CQ), halofantrine (HAL), lopinavir/ritonavir (LOP/RIT), moxifloxacin (MOX) and QUIN simulated in this study were taken from the literature, and are shown in electronic supplementary material, table S1.

Based on the availability of ion channel block data for each compound, changes in up to seven ion currents, namely I_{Kr} , I_{Ks} , I_{K1} , I_{CaL} , I_{NaL} , I_{NaL} , I_{to} , were inputted into the O'Hara-Rudy (ORd) human ventricle mathematical action potential model [29]. For example, based on the values presented in electronic supplementary material, table S1, AZ was assumed to block I_{Kr} , I_{NaL} , I_{Ks} and I_{to} with $\text{IC}_{50\text{s}}$ of 70.8, 189.1, 470.0 and 88.8 μM , respectively. Drug block was modelled using conductance block where a proportion b_i of channel type i are blocked, and the maximal density of the current is then scaled by $(1 - b_i)$ [20]. For simulation of combinations of drugs, the Bliss model of independent block was assumed [30], in which the total proportion of channels blocked arising from the combination of the block by drugs 1 and 2 was given by

$$b_i = b_{1,i} + b_{2,i} - b_{1,i}b_{2,i}. \quad (2.1)$$

That is, block occurs when one compound, the other, or both are bound to an individual channel, and any of these scenarios leads to complete block of an individual channel. Combinations of drugs were applied at plasma concentrations based on the ratio of free C_{max} for drugs from clinical studies referenced in electronic supplementary material, table S1 (where a range is shown, the highest available C_{max} was used). A torsade metric score was calculated for each compound, computed as the average qNet at $1-4 \times C_{\text{max}}$ [28]. Briefly, qNet is a measure of the net charge crossing the membrane during a simulated action potential repolarization, calculated as the integral or area under the curve of a net current, I_{Net} , defined as

$$I_{\text{Net}} = I_{\text{CaL}} + I_{\text{NaL}} + I_{\text{Kr}} + I_{\text{Ks}} + I_{\text{K1}} + I_{\text{to}}. \quad (2.2)$$

A previous study found that estimates of pIC_{50} from repeated ion channel screens followed a logistic form, i.e. $\text{pIC}_{50} \sim \text{logistic}(\mu, \sigma)$ [21], where μ is the mean and σ is a spread parameter. Obtaining a value for σ in each of the affected ion channels allows uncertainty in IC_{50} estimates to be propagated through to APD and qNet predictions. We used previously reported values of σ [21] for I_{Kr} , I_{Ks} , I_{NaL} , I_{CaL} and I_{to} , or a conservative value of 0.15 for ion channels for which this information was not available (I_{NaL} and I_{K1}). A pIC_{50} estimate for each channel of interest was subsequently sampled from the corresponding logistic distribution—a process which was repeated 1000 times for each compound, resulting in 1000 distinct concentration–APD and concentration–qNet response curves. Ignoring the upper and lower 5% of

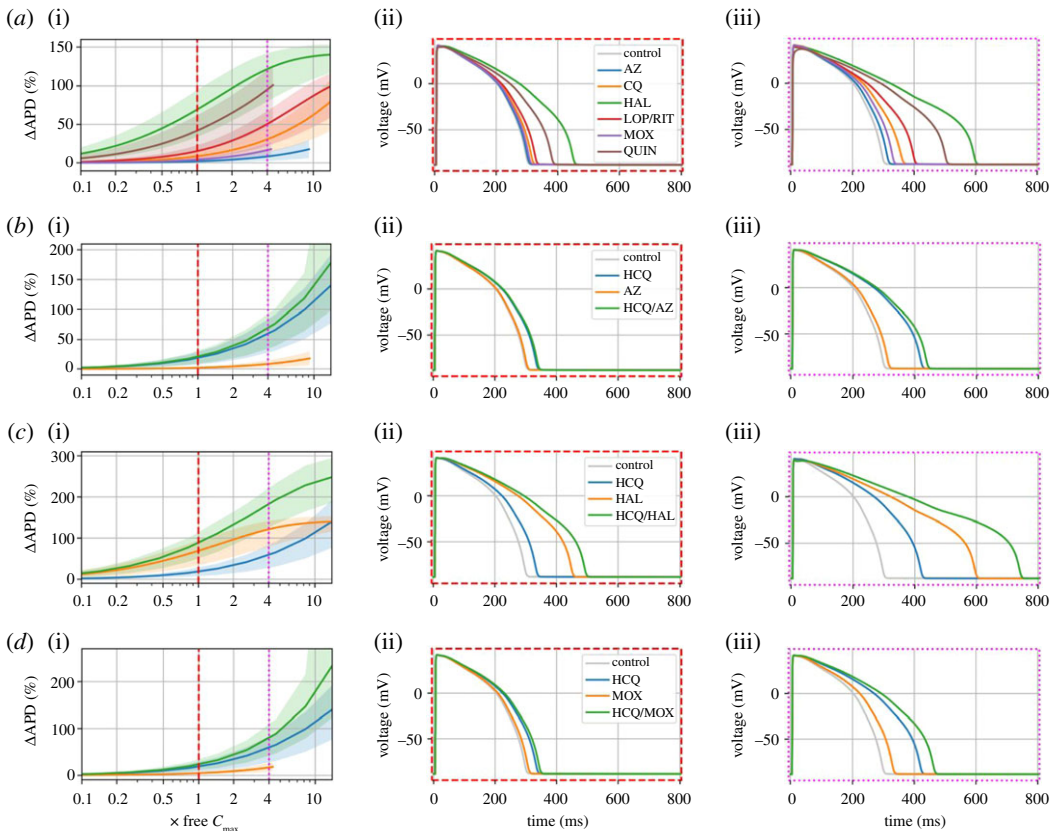


Figure 1. (a)(i) APD–concentration curves with 90% credible intervals from 1000 samples for control and azithromycin (AZ), chloroquine (CQ), halofantrine (HAL), lopinavir/ritonavir (LOP/RIT), moxifloxacin (MOX) and quinine (QUIN), with selected APs at concentrations of $1\times$ free C_{\max} (ii) and $4\times$ free C_{\max} (iii). Combinations of hydroxychloroquine (HCQ) with AZ, HAL and MOX are shown in (b), (c) and (d), respectively.

outputs allowed us to obtain an estimate of the 90% credible interval for simulated response curves. All AP simulations and qNet calculations were performed using ApPredict, a bolt-on extension to Chaste (which also has a web-portal front end [31]). All simulation data and codes required to run the simulations are freely available in the Github repository: <https://github.com/CardiacModelling/risk-stratification-anti-malarials>.

3. Results

In this study, we used increases in the cellular APD as a surrogate for QT interval prolongation [20]. The effects of each of the drugs on the APD were tested at log-spaced concentrations ranging from 0.001 to 100 μM and plotted in terms of the free C_{\max} , in order to measure the % change in APD₉₀ with concentration. The APD₉₀ as a function of concentration is shown for AZ, CQ, HAL, LOP/RIT, MOX and QUIN in figure 1a, with APs at concentrations equivalent to $1\times$ and $4\times$ free C_{\max} highlighted. The compounds investigated generally had a free C_{\max} which is much less than the hERG IC₅₀ and so produced only a small degree of APD prolongation at $1\times$ free C_{\max} , including lopinavir/ritonavir. HAL on the other hand produced substantial APD prolongation at $1\times$ free C_{\max} due to comparable values of hERG IC₅₀ and free C_{\max} . QUIN produced smaller but still substantial APD prolongation at $1\text{--}4\times$ free C_{\max} . At a concentration $4\times$ free C_{\max} , LOP/RIT and CQ also produced fairly substantial APD prolongations, whereas this remained comparatively small for AZ and MOX.

Figure 1b–d shows APD–concentration curves for HCQ and various drugs administered alone, and in combination with HCQ. While the antibiotics AZ and MOX both had very minor APD prolonging effects when administered alone, they were both predicted to increase the overall degree of APD prolongation slightly when given with HCQ compared to HCQ alone. Both HAL and HCQ had a considerable effect when administered individually, so produced a substantial APD prolongation when combined (especially at $4\times$ free C_{\max}).

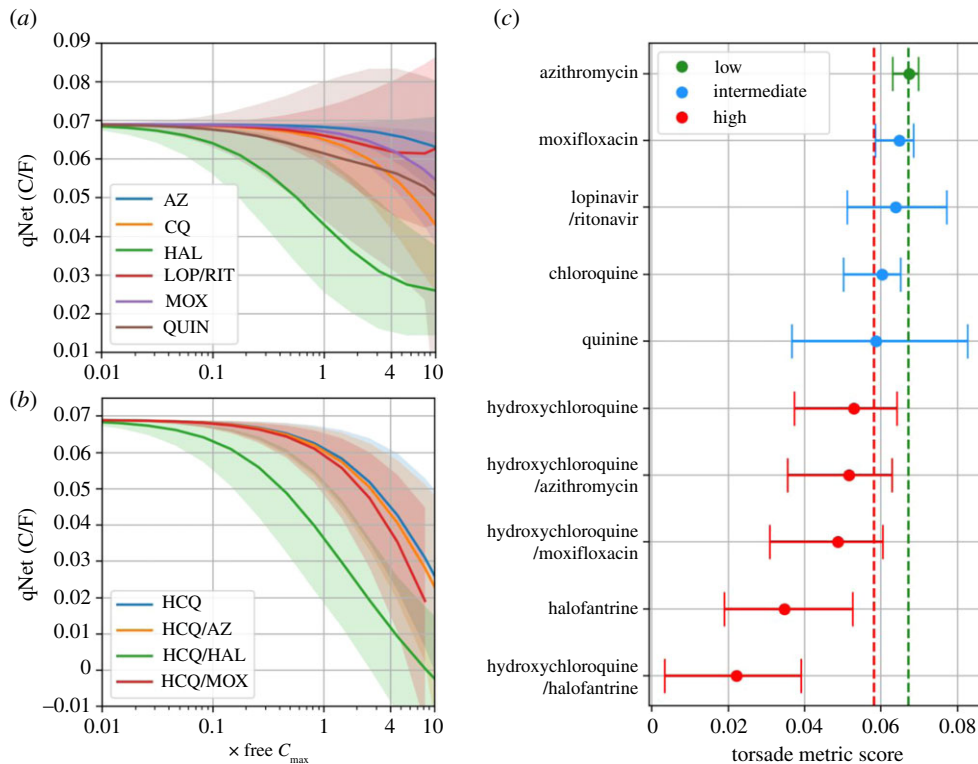


Figure 2. qNet–concentration curves with 90% credible intervals from 1000 samples for (a) azithromycin (AZ), chloroquine (CQ), halofantrine (HAL), lopinavir/ritonavir (LOP/RIT), moxifloxacin (MOX) and quinine (QUIN), and (b) hydroxychloroquine (HCQ), HCQ/AZ, HCQ/HAL and HCQ/MOX. (c) Torsade metric scores for individual compounds and combinations, separated into low, intermediate and high risk based on thresholds in [28], shown as red and green dotted lines.

Figure 2 shows the concentration–qNet curves for individual compounds and drug combinations, as well as associated torsade metric scores. Based on APD prolongation at a concentration of 1–4 \times free C_{\max} in figure 1, one would expect lopinavir/ritonavir to be slightly riskier than CQ. The qNet for CQ at this concentration, however, was lower (riskier) than for lopinavir/ritonavir (figure 2a), highlighting the different information provided by qNet; namely, that the balance of currents leading to APD prolongation is altered in a riskier way for CQ.

AZ was predicted to have the safest (highest) median qNet, yet the uncertainties around lopinavir/ritonavir and QUIN were greater, so they could be the safer compounds/combination. Lopinavir and ritonavir have almost identical hERG IC_{50} s, which also coincide somewhat with the I_{CaL} and I_{NaL} IC_{50} s for ritonavir, all of which would be expected to influence the degree of APD prolongation in the model. Therefore, as the concentration approaches the hERG (and other) IC_{50} values there were several inputs close to the region of maximum uncertainty in the dose–response curve, generating large uncertainty in the output.

Combinations of drugs with HCQ decreased qNet in the order HAL > MOX > AZ (figure 2b). The torsade metric scores shown in figure 2c reveal that HCQ/HAL was predicted to be the riskiest combination of drugs, whereas HAL was predicted to be a highly risky individual drug. At the other end of the scale, AZ was the only compound placed in the low-risk category. However, combining AZ with HCQ resulted in a most likely high-risk outcome. CQ was placed in the intermediate-high-risk category, compared to mostly high risk for HCQ. As a free C_{\max} for HCQ treatment for which plasma binding was taken into account was not available for SLE and/or COVID doses, we used a value associated with a malaria dose [32].

4. Discussion

In this study, we used a previously developed classifier [29] to predict the clinical torsadogenic risk category associated with commonly used anti-malarials and anti-infective agents which prolong the QT interval, as well as an independent block model to assess the safety profile of combination

therapies that block multiple ion channels. These simulations were based on the earliest pre-clinical data available (measurement of IC_{50} s, typically from high-throughput assays), and integrate multi-channel effects to better predict risk classifications of drugs. Drugs such as CQ and HCQ have garnered a lot of attention over many years as they appear to work via multiple mechanisms and hence have shown promise in several disease conditions. Most recently, significant interest in the compounds was shown regarding the treatment and prevention of COVID-19. This interest has waned after cessation of the HCQ arm of the RECOVERY trial [33] and lack of impact, combined with the potential for adverse events [34,35], although support for the use of HCQ, AZ and their combined use continues to appear in recent publications in both the peer-reviewed [36,37] and popular literature [38] and discussions continue as to the merits of adjuvant therapy with zinc supplementation [39,40].

Drug safety requires the ability to predict and assess risk with an acceptable level of certainty including on major target organs [41]. We have taken advantage of recent developments in computational modelling [21,29] and knowledge derived from single-cell electrophysiological measurements of different quinolines (including CQ, HCQ, quinidine, QUIN and HAL) on up to seven major ion currents including I_{Kr} and I_{CaL} to stratify the risk of some of these compounds both individually and in combination with other compounds. Furthermore, as such models require increased scrutiny for use in safety-critical applications [19], we have performed uncertainty quantification. Our modelling showed that combining HCQ with AZ prolonged APD to a greater extent than the use of either individually (albeit this was notable only at $4\times$ free C_{max}), and placed this combination in the high-risk category associated with measurable/unacceptable incidence of TdP. Furthermore, combining HCQ with MOX or HAL was also predicted to increase TdP risk.

Data in animal models have previously shown HCQ to have multi-channel actions including on calcium and potassium currents [16]. It is known that concurrent block of calcium currents with I_{Kr} inhibition can protect against TdP and our modelling data suggest this is indeed the case for many compounds, including HCQ at low concentrations. Modelling results for a free C_{max} of approximately $1.2\ \mu\text{M}$ indicated that the balance of potassium and calcium current inhibitions observed would not be expected to lengthen the human ventricular action potential significantly at a dose of $1\times$ free C_{max} (figure 1), but did so at $4\times$ free C_{max} , which resulted in an overall high-intermediate-risk category for HCQ. However, we also showed that accounting for variability in our experimental data led to a range of possibilities. With the exception of HAL and HCQ/HAL, all compounds and combinations investigated produced credible intervals for the torsade metric score that spanned at least two risk categories. Gathering more high-quality experimental data regarding the multi-channel inhibition effects of HCQ and other anti-malarials would allow us to predict with more confidence the most plausible APD prolongation range and risk category. We could also have accounted for different Hill coefficients, although it has been noted previously that the associated level of variability in their measurement is so high that it is unclear whether including the Hill coefficient from ion channel screening adds useful information [21]. It should be noted, in addition, that the IC_{50} used as a model input has limitations as a measure of drug block, in that its value may depend on the electrophysiology protocol used [42,43], and, relatedly, it is unable to account for dynamic, state-dependent effects of a compound. Recent studies have integrated dynamic effects into computational models through the use of drug-binding kinetic schemes with rates inferred from specialized electrophysiology protocols [29] and atomistic scale measurements [44].

Our modelling predicted that CQ at a free C_{max} of approximately $0.7\ \mu\text{M}$ was generally safer than HCQ at a free C_{max} of approximately $1.2\ \mu\text{M}$ (used in the treatment of malaria at 400 mg [32]; figure 2). However, it should be noted that the free C_{max} for HCQ is approximately 2 times greater than that for CQ; if the same free C_{max} is used for both compounds then the risk scores are comparable (electronic supplementary material, figure S1). High doses of CQ are thus still expected to pose a high risk. Furthermore, the free C_{max} we used for HCQ was for a malaria dose, which is a higher dose than for SLE. We expect that HCQ at the lower doses used for SLE thus remains generally safe (towards the intermediate-risk category), whereas higher doses used for COVID-19 will place HCQ unequivocally in the high-risk category (electronic supplementary material, figure S1). This is in keeping with clinical experience where CQ and HCQ are known to cause sudden death in overdose but have an otherwise good safety record in the treatment of malaria and SLE, respectively [15].

The risk categories presented in this study are based on a combination of adverse events, case reports and clinical judgement by an expert panel, more information about which can be found on the CiPA website [45]. The categories should not be interpreted as the risk of developing TdP when taking a particular compound (which would suggest that someone taking HCQ is at high risk of developing TdP), but rather the likelihood with which TdP that arises in a patient (which may remain extremely

rare) can be attributed to a particular compound. To put some of the risk categories in context, they are compared to quinidine (which has known TdP risk) in electronic supplementary material, figure S2. The torsade metric score (correctly) identified quinidine as high risk, suggesting that it is highly probable that TdP can be attributed to quinidine in cases where it arises in patients (far more so than for other compounds tested), which is consistent with clinical experience and the known safety profile of quinidine.

A comparison of the results in this study with risk scores/categories from previous classifiers and databases (where available) is shown in electronic supplementary material, table S2. While it is hard to compare directly these scores, it can be seen that there is reasonable agreement across the different classification systems regarding which drugs are risky, such as quinidine and HAL, and which drugs pose less of a TdP risk, such as QUIN. This suggests that the qNet metric may capture to a reasonable degree relative differences between compounds in the cellular-level mechanisms that determine TdP. Nonetheless, some discrepancies are apparent. One reason for this is that our model predictions are highly sensitive to the free C_{\max} input. This is not ideal as effective free therapeutic plasma concentrations are not easily obtained from the literature. A final crucial point regarding the classifier is that risk category prediction does not necessarily rely on accurate prediction of APD prolongation [20] and indeed it has been tested for predictions without considering APD [28]; as such, here we use the same classifier to assess cardiac risk while making no claims about the accuracy of the degree of APD prolongation in the model. Further, while we have searched the literature for ion channel blocking effects of the listed compounds, we acknowledge that many compounds have active metabolites and that any potential impact of these upon APD has not been modelled in this analysis.

Patient risk factors can also predispose to cardiotoxicity, some of which may be more common in COVID-19, e.g. electrolyte imbalances, renal failure, drug interactions. COVID-19 also appears to affect the heart (e.g. myocarditis), which may additionally increase cardiotoxicity risk [46]. COVID-19 is also associated with acute kidney injury and electrolyte abnormalities [47]. Safety of drug–drug interactions (including combinations of anti-malarials) are an important consideration when being explored as a therapeutic in comorbid patients [48].

5. Conclusion

The safety profile of both CQ and HCQ are well-established. Since the SARS-CoV-2 outbreak, the ability of CQ/HCQ to inhibit certain coronaviruses has been explored. Although interest in HCQ use for acutely unwell COVID-19 patients has waned, there is a continued interest in potential use at symptom onset or as a prophylactic, with combination therapies with zinc and/or AZ under continued discussion in peer-reviewed and popular literature. In this study, we demonstrate an *in silico* safety assessment with uncertainty quantification based on the CiPA qNet torsade metric score. At a free C_{\max} of approximately 1.2 μM as seen in malaria treatment, HCQ would most likely be placed in the high-intermediate-risk category for TdP arrhythmia, whereas CQ was predicted to most likely lie in the intermediate-risk category at a free C_{\max} of approximately 0.7 μM . Combining HCQ with the antibacterial MOX, or the anti-malarial HAL was predicted to increase risk compared to administration of HCQ alone, increasing the degree of human ventricular APD prolongation at some or all concentrations investigated. Further clinical work will be required in order to assess the cardiac effects of HCQ at different doses as used in specific disease populations.

Data accessibility. The data underlying this article are available on Github in the following repository: <https://github.com/CardiacModelling/risk-stratification-anti-malarials>. All simulation data and codes required to run the simulations are freely available in Github: <https://github.com/CardiacModelling/risk-stratification-anti-malarials> and have been archived within the Zenodo repository: <https://doi.org/10.5281/zenodo.4650300>.

Authors' contributions. D.G.W.: designed experiments, conducted experiments, data analysis, contributed to manuscript writing. R.A.C.: conducted experiments, contributed to manuscript writing. M.H.: contributed to experiments. X.H.S.C., N.J.W. and N.H.: contributed to manuscript writing and data interpretation. G.R.M. and R.-A.B.B.: conceived the idea, drafted the manuscript, contributed to data analysis and data interpretation.

Competing interests. We declare we have no competing interests.

Funding. This work was supported by the Wellcome Trust and Royal Society (grant no. 109371/Z/15/Z); the British Heart Foundation (grant nos. PG/18/4/33521 and FS/15/8/3115); the Wellcome Trust (grant no. 212203/Z/18/Z); and the BHF Centre of Research Excellence (grant no. RE/08/004). R.-A.B.B. and R.A.C. acknowledge support from a Sir Henry Dale Wellcome Trust and Royal Society fellowship, and R.-A.B.B. acknowledges support from The Returning Carers' Fund, Medical Sciences Division, University of Oxford and the British Heart Foundation. G.R.M. and D.G.W. acknowledge support from the Wellcome Trust via a Wellcome Trust Senior Research

References

- Ponticelli C, Moroni G. 2017 Hydroxychloroquine in systemic lupus erythematosus (SLE). *Expert Opin. Drug Saf.* **16**, 411–419. (doi:10.1080/14740338.2017.1269168)
- Noujaim SF, Stuckey JA, Ponce-Balbuena D, Ferrer-Villada T, López-Izquierdo A, Pandit SV, Sanchez-Chapula JA, Jalife J. 2011 Structural bases for the different anti-fibrillatory effects of chloroquine and quinidine. *Cardiovasc. Res.* **89**, 862–869. (doi:10.1093/cvr/cvr008)
- Surrey AR, Hammer HF. 1950 The preparation of 7-Chloro-4-(4-(N-ethyl-N-β-hydroxyethylamino)-1-methylbutylamino)-quinoline and related compounds. *J. Am. Chem. Soc.* **72**, 1814–1815. (doi:10.1021/ja01160a116)
- Hoekenga MT. 1955 The treatment of malaria with hydroxychloroquine. *Am. J. Trop. Med. Hyg.* **4**, 221–223. (doi:10.4269/ajtmh.1955.4.221)
- Burrell ZL, Martinez AC. 1958 Chloroquine and hydroxychloroquine in the treatment of cardiac arrhythmias. *N. Engl. J. Med.* **258**, 798–800. (doi:10.1056/NEJM195804172581608)
- Sumpter M, Tatro L, Stoecker W, Rader R. 2012 Evidence for risk of cardiomyopathy with hydroxychloroquine. *Lupus* **21**, 1594–1596. (doi:10.1177/0961203312462757)
- Durcan L, Clarke WA, Magder LS, Petri M. 2015 Hydroxychloroquine blood levels in SLE: clarifying dosing controversies and improving adherence. *J. Rheumatol.* **42**, 2092–2097. (doi:10.3899/jrheum.150379)
- Ben-Zvi I, Kivity S, Langevitz P, Shoenfeld Y. 2012 Hydroxychloroquine: from malaria to autoimmunity. *Clin. Rev. Allergy Immunol.* **42**, 145–153. (doi:10.1007/s12016-010-8243-x)
- Browning DJ. 2014 Pharmacology of chloroquine and hydroxychloroquine. In *Hydroxychloroquine and chloroquine retinopathy* (ed. DJ Browning), pp. 35–63. New York, NY: Springer.
- Costedoat-Chalumeau N *et al.* 2015 A critical review of the effects of hydroxychloroquine and chloroquine on the eye. *Clin. Rev. Allergy Immunol.* **49**, 317–326. (doi:10.1007/s12016-015-8469-8)
- Costedoat-Chalumeau N *et al.* 2003 Safety of hydroxychloroquine in pregnant patients with connective tissue diseases: a study of one hundred thirty-three cases compared with a control group. *Arthritis Rheum.* **48**, 3207–3211. (doi:10.1002/art.11304)
- Hydroxychloroquine (Plaquenil) [Internet]. [cited 14 April 2020]. See <https://www.rheumatology.org/I-Am-A/Patient-Caregiver/Treatments/Hydroxychloroquine-Plaquenil>.
- Medications used to treat lupus | Lupus Foundation of America [Internet]. [cited 14 April 2020]. See <https://www.lupus.org/resources/medications-used-to-treat-lupus>.
- Verbaanderd C, Maes H, Schaaf MB, Sukhatme VP, Pantziarka P, Sukhatme V, Agostinis P, Bouche G. 2017 Repurposing drugs in oncology (ReDO)—chloroquine and hydroxychloroquine as anti-cancer agents. *ecancer* **11**, 781. (doi:10.3332/ecancer.2017.781)
- Haeusler IL, Chan XHS, Guérin PJ, White NJ. 2018 The arrhythmogenic cardiotoxicity of the quinoline and structurally related antimalarial drugs: a systematic review. *BMC Med.* **16**, 200. (doi:10.1186/s12916-018-1188-2)
- Capel RA *et al.* 2015 Hydroxychloroquine reduces heart rate by modulating the hyperpolarization-activated current *I_f*: novel electrophysiological insights and therapeutic potential. *Heart Rhythm.* **12**, 2186–2194. (doi:10.1016/j.hrthm.2015.05.027)
- Noble D. 1962 A modification of the Hodgkin-Huxley equations applicable to Purkinje fibre action and pacemaker potentials. *J. Physiol.* **160**, 317–352. (doi:10.1113/jphysiol.1962.sp006849)
- Whittaker DG, Clerx M, Lei CL, Christini DJ, Mirams GR. 2020 Calibration of ionic and cellular cardiac electrophysiology models. *WIREs Syst. Biol. Med.* **12**, e1482. (doi:10.1002/wsbm.1482)
- Mirams GR, Niederer SA, Clayton RH. 2020 The fickle heart: uncertainty quantification in cardiac and cardiovascular modelling and simulation. *Phil. Trans. R. Soc. Math. Phys. Eng. Sci.* **378**, 20200119. (doi:10.1098/rsta.2020.0119)
- Mirams GR, Cui Y, Sher A, Fink M, Cooper J, Heath BM, McMahon NC, Gavaghan DJ, Noble D. 2011 Simulation of multiple ion channel block provides improved early prediction of compounds' clinical torsadogenic risk. *Cardiovasc. Res.* **91**, 53–61. (doi:10.1093/cvr/cvr044)
- Elkins RC, Davies MR, Brough SJ, Gavaghan DJ, Cui Y, Abi-Gerges N, Mirams GR. 2013 Variability in high-throughput ion-channel screening data and consequences for cardiac safety assessment. *J. Pharmacol. Toxicol. Methods.* **68**, 112–122. (doi:10.1016/j.vascn.2013.04.007)
- Chang KC *et al.* 2017 Uncertainty quantification reveals the importance of data variability and experimental design considerations for *in silico* proarrhythmia risk assessment. *Front. Physiol.* **8**, 917. (doi:10.3389/fphys.2017.00917)
- Jervell A, Lange-Nielsen F. 1957 Congenital deaf-mutism, functional heart disease with prolongation of the Q-T interval, and sudden death. *Am. Heart J.* **54**, 59–68. (doi:10.1016/0002-8703(57)90079-0)
- El-Sherif N, Turitto G, Boutjdir M. 2018 Acquired long QT syndrome and torsade de pointes. *Pacing Clin. Electrophysiol.* **41**, 414–421. (doi:10.1111/pace.13296)
- El-Sherif N, Turitto G. 2011 Electrolyte disorders and arrhythmogenesis. *Cardiol. J.* **18**, 233–245.
- Kannankeril P, Roden DM, Darbar D. 2010 Drug-induced long QT syndrome. *Pharmacol. Rev.* **62**, 760–781. (doi:10.1124/pr.110.003723)
- Redfern WS *et al.* 2003 Relationships between preclinical cardiac electrophysiology, clinical QT interval prolongation and torsade de pointes for a broad range of drugs: evidence for a provisional safety margin in drug development. *Cardiovasc. Res.* **58**, 32–45. (doi:10.1016/S0008-6363(02)00846-5)
- Li Z *et al.* 2019 Assessment of an *in silico* mechanistic model for proarrhythmia risk prediction under the GPA initiative. *Clin. Pharmacol. Ther.* **105**, 466–475. (doi:10.1002/cpt.1184)
- Li Z *et al.* 2017 Improving the *in silico* assessment of proarrhythmia risk by combining hERG (human Ether-à-go-go-Related Gene) channel–drug binding kinetics and multichannel pharmacology. *Circ. Arrhythm. Electrophysiol.* **10**, e004628. (doi:10.1161/CIRCEP.116.004628)
- Bliss CI. 1939 The toxicity of poisons applied jointly. *Ann. Appl. Biol.* **26**, 585–615. (doi:10.1111/j.1744-7348.1939.tb06990.x)
- Williams G, Mirams GR. 2015 A web portal for *in-silico* action potential predictions. *J. Pharmacol. Toxicol. Methods.* **75**, 10–16. (doi:10.1016/j.vascn.2015.05.002)
- Lim H-S *et al.* 2009 Pharmacokinetics of hydroxychloroquine and its clinical implications in chemoprophylaxis against malaria caused by *Plasmodium vivax*. *Antimicrob. Agents Chemother.* **53**, 1468–1475. (doi:10.1128/AAC.00339-08)
- No clinical benefit from use of hydroxychloroquine in hospitalised patients with COVID-19—RECOVERY Trial. [cited 8 February 2021]. See <https://www.recoverytrial.net/news/statement-from-the-chief-investigators-of-the-randomised-evaluation-of-covid-19-therapy-recovery-trial-on-hydroxychloroquine-5-june-2020-no-clinical-benefit-from-use-of-hydroxychloroquine-in-hospitalised-patients-with-covid-19>.
- Magagnoli J *et al.* 2020 Outcomes of hydroxychloroquine usage in United States veterans hospitalized with COVID-19. *Med* **1**, 114–127.e3.
- Borba MGS *et al.* 2020 Effect of high vs low doses of chloroquine diphosphate as adjunctive therapy for patients hospitalized with severe acute respiratory syndrome coronavirus 2 (SARS-CoV-2) infection: a randomized clinical trial. *JAMA Netw. Open* **3**, e208857. (doi:10.1001/jamanetworkopen.2020.8857)
- McCullough PA *et al.* 2021 Pathophysiological basis and rationale for early outpatient treatment of SARS-CoV-2 (COVID-19) infection. *Am. J. Med.* **134**, 16–22. (doi:10.1016/j.amjmed.2020.07.003)
- Lauriola M *et al.* 2020 Effect of combination therapy of hydroxychloroquine and azithromycin on mortality in patients with COVID-19. *Clin. Transl. Sci.* **13**, 1071–1076. (doi:10.1111/cts.12860)

38. bulle. Journal of Medicine Says HCQ+Zinc Reduces COVID Deaths [Internet]. [cited 8 February 2021]. See <https://mindbodyhealthiness.com/index.php/2021/02/01/journal-of-medicine-says-hcq-zinc-reduces-covid-deaths/>.
39. Abd-Elsalam S *et al.* 2020 Do zinc supplements enhance the clinical efficacy of hydroxychloroquine? A randomized, multicenter trial. *Biol. Trace Elem. Res.* (online ahead of print). (doi:10.1007/s12011-020-02512-1)
40. Derwand R, Scholz M, Zelenko V. 2020 COVID-19 outpatients: early risk-stratified treatment with zinc plus low-dose hydroxychloroquine and azithromycin: a retrospective case series study. *Int. J. Antimicrob. Agents.* **56**, 106214. (doi:10.1016/j.ijantimicag.2020.106214)
41. Weaver RJ, Valentin J-P. 2019 Today's challenges to de-risk and predict drug safety in human 'Mind-the-Gap'. *Toxicol. Sci.* **167**, 307–321. (doi:10.1093/toxsci/kfy270)
42. Lee W, Windley MJ, Perry MD, Vandenberg JJ, Hill AP. 2019 Protocol-dependent differences in IC50 values measured in human ether-á-go-go-related gene assays occur in a predictable way and can be used to quantify state preference of drug binding. *Mol. Pharmacol.* **95**, 537–550. (doi:10.1124/mol.118.115220)
43. Gomis-Tena J, Brown BM, Cano J, Trenor B, Yang P-C, Saiz J, Clancy CE, Romero L. 2020 When does the IC₅₀ accurately assess the blocking potency of a drug? *J. Chem. Inf. Model.* **60**, 1779–1790. (doi:10.1021/acs.jcim.9b01085)
44. Yang P-C *et al.* 2020 A computational pipeline to predict cardiotoxicity. *Circ. Res.* **126**, 947–964. (doi:10.1161/CIRCRESAHA.119.316404)
45. CiPA. 2020 [Internet]. [cited 4 August 2020]. See <https://cipaproject.org/>.
46. Lazzarini PE, Boutjdir M, Capecchi PL. 2020 COVID-19, arrhythmic risk and inflammation: mind the gap! *Circulation* **142**, 7–9. (doi:10.1161/CIRCULATIONAHA.120.047293)
47. Ronco C, Reis T, Husain-Syed F. 2020 Management of acute kidney injury in patients with COVID-19. *Lancet Respir. Med.* **8**, 738–742. (doi:10.1016/S2213-2600(20)30229-0)
48. Ngoro X, Tobeka N, Aderibigbe BA. 2017 Quinoline-based hybrid compounds with antimalarial activity. *Mol. J. Synth. Chem. Nat. Prod. Chem.* **22**, 2268. (doi:10.3390/molecules22122268)

Cardiac TdP Risk Stratification Modelling of Anti-Infective Compounds including Chloroquine and Hydroxychloroquine

Supplemental Material

Dominic G. Whittaker, Rebecca A. Capel, Maurice Hendrix, Xin Hui S. Chan, Neil Herring, Nicholas J. White, Gary R. Mirams, Rebecca-Ann B. Burton

Table S1: A summary of IC_{50s} (μM) and effective free therapeutic plasma concentrations (free C_{max}; μM) for different anti-malarial compounds using values from the literature.

	hERG	Cav1.2	Nav1.5 (peak)	Nav1.5 (late)	KvLQT1 /minK	Kv4.3	Kir2.1	Free C_{max}
Azithromycin [1], [2]	70.8	-	-	189.1	470	88.8	-	0.4 – 1.937
CQ [1], [3], [4]	6.89	-	-	-	-	-	10.60	0.2495 – 0.66
Halofantrine [3], [5]	0.38	1.9	331.2	-	-	-	-	0.172 – 0.57
HCQ [6], [7]	5.62	26.9			9.33			1.22
Lopinavir [1]	5.17	15.6	-	-	-	-	-	0.704
Moxifloxacin [1], [2]	93.0	-	-	382.3	50.3	-	-	3.5 – 4.111
Ritonavir [1]	5.16	8.23	-	7.18	-	-	-	0.437
Quinidine [1]	0.34				4.90			0.8429 – 3.237
Quinine [1], [4]	5.17	27.18	24.15	11.05	37.45	79.25	-	1.83 – 3.9567

Dashes mean that no effect was measured, whereas blank spaces mean that no measurement was made.

Table S2: A comparison of risk categories/scores from a range of TdP risk metrics.

	Miramis [8]	Harmer QRS [4]	Redfern [9]	Credible Meds [10]	Kramer [5]	qNet (this study) [11]
Azithromycin	4			KR		Low
Chloroquine	3	2	4	KR		Intermediate
Halofantrine	4		3	KR	TdP+	High
Hydroxychloroquine	4			KR		High
Lopinavir/ritonavir				PR		Intermediate
Moxifloxacin	4	3		KR	TdP+	Intermediate
Quinidine	1	1	1	KR	TdP+	High
Quinine	4	2		CR		Intermediate

Abbreviations for Credible Meds are as follows: CR (conditional risk); KR (known risk); possible risk (PR). For the Harmer risk score, the numbers correspond to: (1) Class I anti-arrhythmics; (2) QRS prolonging drugs; (3) Non-QRS prolonging drugs. The Miramis/Redfern categories correspond to: (1) Class Ia and III anti-arrhythmics; typically associated with a considerable, but acceptable, risk of TdP; (2) Drugs that have been withdrawn from the market due to unacceptable TdP risk; (3) Drugs with a measurable incidence of TdP, or for which numerous case reports exist; (4) Drugs for which there have been isolated case reports of TdP; (5) Drugs for which there have been no published reports of TdP. For the Kramer category, TdP+ denotes a compound that was predicted to be torsadogenic.

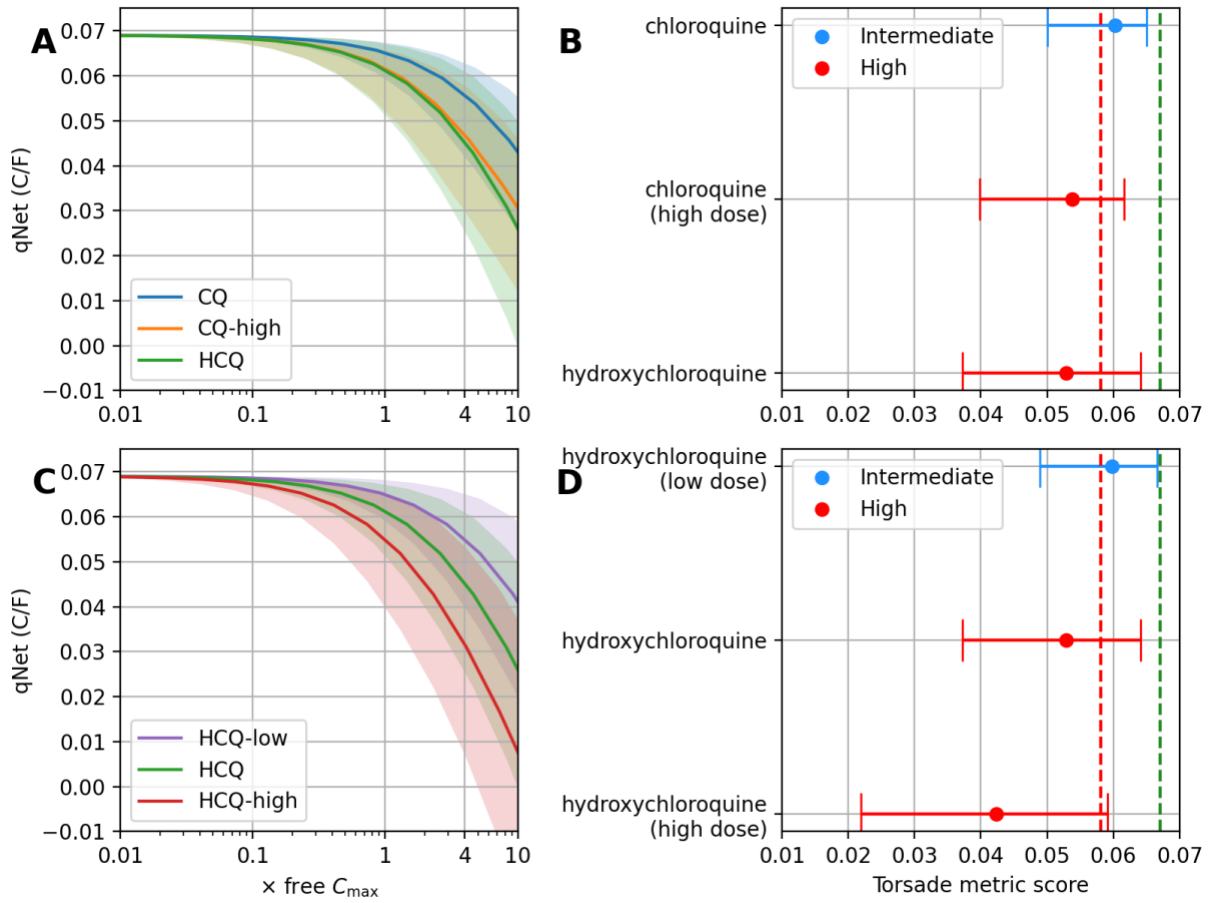


Figure S1: $qNet$ -concentration curves with 90% credible intervals from 1000 samples for (A) chloroquine (CQ), at normal and high ($2\times$) dose (relative to the default malaria dose used), and hydroxychloroquine (HCQ), and (C) HCQ at normal, low ($0.5\times$), and high doses ($2\times$) (relative to the default malaria dose used). Corresponding torsade metric scores for CQ (B) and HCQ (D), separated into low, intermediate, and high risk based on thresholds in [12].

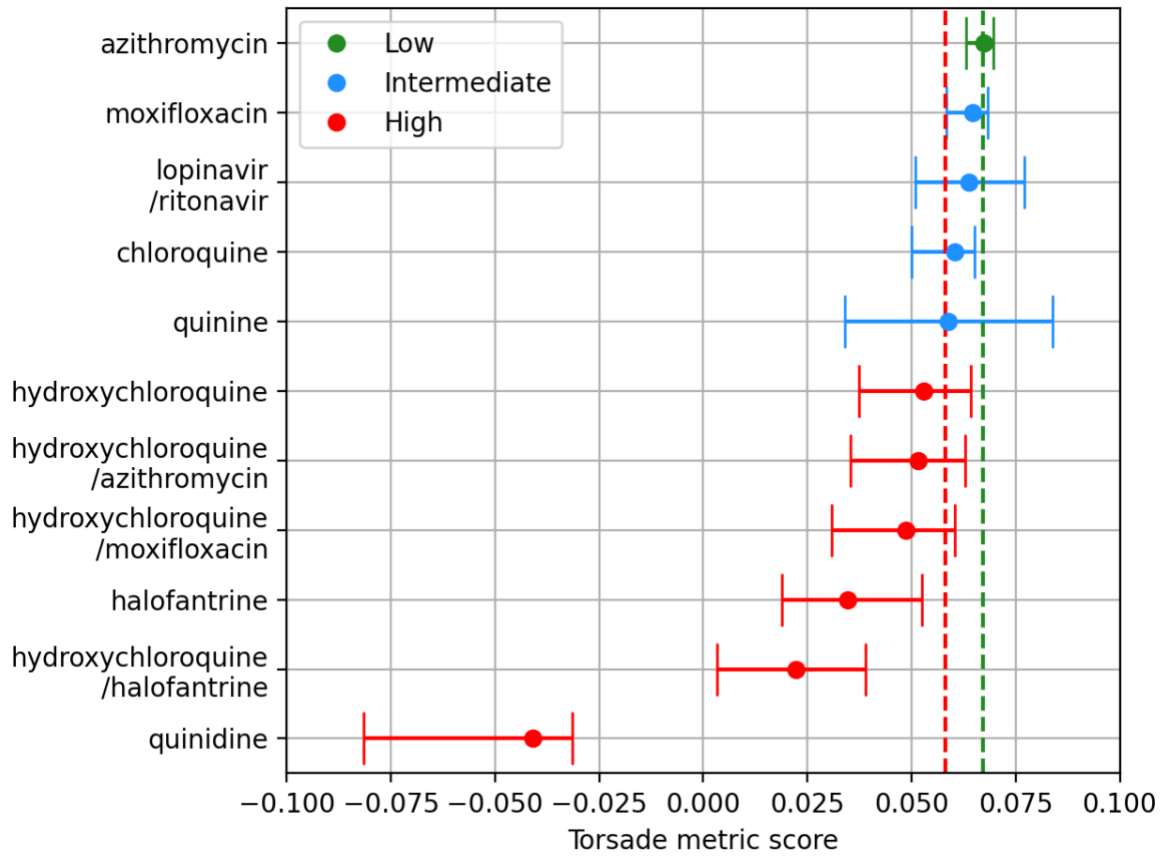


Figure S2: Torsade metric scores for individual compounds and combinations, separated into low, intermediate, and high risk based on thresholds in [12], shown as red and green dotted lines. Quinidine is included for comparison.

References

- [1] W. J. Crumb, J. Vicente, L. Johannesen, and D. G. Strauss, 'An evaluation of 30 clinical drugs against the comprehensive in vitro proarrhythmia assay (CiPA) proposed ion channel panel', *J. Pharmacol. Toxicol. Methods*, vol. 81, pp. 251–262, Sep. 2016, doi: 10.1016/j.vascn.2016.03.009.
- [2] C. L. Lawrence, M. H. Bridgland-Taylor, C. E. Pollard, T. G. Hammond, and J.-P. Valentin, 'A rabbit Langendorff heart proarrhythmia model: predictive value for clinical identification of Torsades de Pointes', *Br. J. Pharmacol.*, vol. 149, no. 7, pp. 845–860, Dec. 2006, doi: 10.1038/sj.bjp.0706894.
- [3] F. Borsini *et al.*, 'In Vitro Cardiovascular Effects of Dihydroartemisinin-Piperaquine Combination Compared with Other Antimalarials', *Antimicrob. Agents Chemother.*, vol. 56, no. 6, pp. 3261–3270, Jun. 2012, doi: 10.1128/AAC.05688-11.
- [4] A. Harmer, J.-P. Valentin, and C. Pollard, 'On the relationship between block of the cardiac Na⁺ channel and drug-induced prolongation of the QRS complex', *Br. J. Pharmacol.*, vol. 164, no. 2, pp. 260–273, Sep. 2011, doi: 10.1111/j.1476-5381.2011.01415.x.
- [5] J. Kramer *et al.*, 'MICE Models: Superior to the HERG Model in Predicting Torsade de Pointes', *Sci. Rep.*, vol. 3, Jul. 2013, doi: 10.1038/srep02100.
- [6] R. A. Capel *et al.*, 'Hydroxychloroquine reduces heart rate by modulating the hyperpolarization-activated current I_f: Novel electrophysiological insights and therapeutic potential', *Heart Rhythm*, vol. 12, no. 10, pp. 2186–2194, Oct. 2015, doi: 10.1016/j.hrthm.2015.05.027.
- [7] H.-S. Lim *et al.*, 'Pharmacokinetics of Hydroxychloroquine and Its Clinical Implications in Chemoprophylaxis against Malaria Caused by Plasmodium vivax', *Antimicrob. Agents Chemother.*, vol. 53, no. 4, pp. 1468–1475, Apr. 2009, doi: 10.1128/AAC.00339-08.
- [8] G. R. Mirams *et al.*, 'Simulation of multiple ion channel block provides improved early prediction of compounds' clinical torsadogenic risk', *Cardiovasc. Res.*, vol. 91, no. 1, pp. 53–61, Jul. 2011, doi: 10.1093/cvr/cvr044.
- [9] W. S. Redfern *et al.*, 'Relationships between preclinical cardiac electrophysiology, clinical QT interval prolongation and torsade de pointes for a broad range of drugs: evidence for a provisional safety margin in drug development', *Cardiovasc. Res.*, vol. 58, no. 1, pp. 32–45, Apr. 2003, doi: 10.1016/S0008-6363(02)00846-5.
- [10] 'CredibleMeds :: Home'. <https://www.crediblemeds.org/> (accessed Aug. 04, 2020).
- [11] Z. Li *et al.*, 'Improving the In Silico Assessment of Proarrhythmia Risk by Combining hERG (Human Ether-à-go-go-Related Gene) Channel–Drug Binding Kinetics and Multichannel Pharmacology', *Circ. Arrhythm. Electrophysiol.*, vol. 10, no. 2, p. e004628, Feb. 2017, doi: 10.1161/CIRCEP.116.004628.
- [12] Z. Li *et al.*, 'Assessment of an In Silico Mechanistic Model for Proarrhythmia Risk Prediction Under the CiPA Initiative', *Clin. Pharmacol. Ther.*, vol. 105, no. 2, pp. 466–475, 2019, doi: 10.1002/cpt.1184.